

arXiv:2305.00675v4 [cs.CV] 13 May 2023

End-to-End Lane detection with One-to-Several Transformer

Kunyang Zhou¹
 kunyangzhou@seu.edu.cn

Rui Zhou²
 2130110210@stmail.ntu.edu.cn

¹ Southeast University
 Nanjing, China

² Nantong University
 Nantong, China

Abstract

Although lane detection methods have shown impressive performance in real-world scenarios, most of methods require post-processing which is not robust enough. Therefore, end-to-end detectors like DEtection TRansformer(DETR) have been introduced in lane detection. However, one-to-one label assignment in DETR can degrade the training efficiency due to label semantic conflicts. Besides, positional query in DETR is unable to provide explicit positional prior, making it difficult to be optimized. In this paper, we present the One-to-Several Transformer(O2SFormer)¹. We first propose the one-to-several label assignment, which combines one-to-many and one-to-one label assignment to solve label semantic conflicts while keeping end-to-end detection. To overcome the difficulty in optimizing one-to-one assignment. We further propose the layer-wise soft label which dynamically adjusts the positive weight of positive lane anchors in different decoder layers. Finally, we design the dynamic anchor-based positional query to explore positional prior by incorporating lane anchors into positional query. Experimental results show that O2SFormer with ResNet50 backbone achieves 77.83% F1 score on CULane dataset, outperforming existing Transformer-based and CNN-based detectors. Furthermore, O2SFormer converges 12.5× faster than DETR for the ResNet18 backbone.

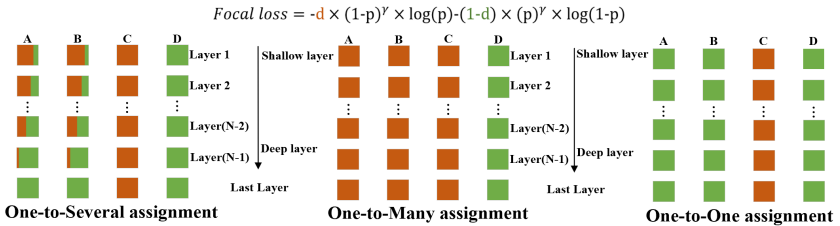


Figure 1: The positive and negative weights of different lane anchors(A,B,C and D) in the classification loss(such as focal loss [13]) across different decoder layers. Each lane anchor has a positive weight d (in brown color) and a negative weight $1-d$ (in green color). C is a fully positive lane anchor, D is a fully negative lane anchor. A and B have the similar label semantic as C. In one-to-one(o2o) assignment, A and B are assigned as negative lane anchor, which leads to label semantic conflicts. While in one-to-many(o2m) assignment, A and B are assigned as positive lane anchor, which requires post-processing to remove duplicate predictions. Moreover, in o2o and o2m assignment, the positive weights for all lane anchors are fixed. In our one-to-several assignment, the positive weights of A and B are dynamically adjusted according to the decoder layers.

¹Code: <https://github.com/zkyseu/O2SFormer>

1 Introduction

Lane detection is a fundamental yet challenging task in computer vision [1, 24, 30], which plays an important role in many applications, such as lane keeping, adaptive cruise control and driving route planning. Recently, many studies [5, 16, 31, 36] focus on using convolutional neural networks (CNNs) for lane detection, which are significantly superior to traditional methods [4, 13, 25] in performance. Nevertheless, most of the state-of-the-art lane detection methods [17, 28, 32] depend on post-processing operations, such as non-maximum suppression (NMS). NMS is not robust enough and difficult to optimize [22]. In addition, due to the limitation of receptive field, CNNs have no advantage in capturing long-range dependence, leading to inefficient feature learning.

DETR [2] is an end-to-end object detector based on Transformer, which treats object detection as a set prediction problem. The self-attention module in Transformer enables DETR to capture long-range dependence better than CNNs. Although there have been several attempts [9, 19] to employ DETR in lane detection, existing methods need either the camera parameters [19] or an additional object detector [9], which hinders the generalization and flexibility of DETR. On the other hand, directly applying DETR to lane detection results in slow convergence and significant performance gaps compared to CNNs. We attribute reasons to two main factors: (1) the positional query in DETR lacks a clear focus area [23], making it difficult for the decoder to locate thin and elongated lanes, and (2) the one-to-one label assignment causes low training efficiency due to label semantic conflicts (as seen in Fig. 1).

In this paper, we propose One-to-Several Transformer(O2SFormer) to address the aforementioned issues. Firstly, to explore explicit positional prior for the positional query, we design the dynamic anchor-based positional query, where lane anchors are encoded as positional query. We update lane anchors layer-by-layer to improve the localization accuracy of lane anchors. Next, we introduce the One-to-Several (O2S) label assignment to solve label semantic conflicts, which combines one-to-many and one-to-one assignment. As illustrated in Fig. 1, we utilize one-to-many assignment for the first N-1 decoder layers and one-to-one assignment for the last layer. Due to the varying learning capabilities of different decoder layers, assigning the same positive weight to all positive lane anchors in the first N-1 decoder layers would make it difficult to optimize the one-to-one assignment. Therefore, we further propose the layer-wise soft label. We assign soft labels with high positive weights to positive lane anchors in the shallow layers of the decoder to improve the discrimination of feature representation, while assigning soft labels with low positive weights to positive lane anchors in the deep layers of the decoder to emphasize end-to-end detection. By adopting the layer-wise soft label, we achieve a better balance between one-to-many and one-to-one assignment.

In summary, the contributions of this paper are summarized as follows.

- We design a novel one-to-several label assignment which combines the advantages of one-to-one and one-to-many assignment to alleviate label semantic conflicts while keeping end-to-end detection. Moreover, we propose the layer-wise soft label to balance one-to-one and one-to-many assignment.
- We present a novel dynamic anchor-based positional query to explore explicit positional prior, which encodes lane anchors as positional queries and updates lane anchors layer-by-layer.
- We evaluate the O2SFormer on the CULane dataset. Experimental results show that O2SFormer accelerates DETR training and achieves better performance than Transformer-based and CNN-based detectors.

2 Related Work

2.1 Lane detection

Deep learning-based lane detection can be divided into three categories according to the representation of lane: segmentation-based method, anchor-based method, and parameter-based method. Segmentation-based methods [26, 52, 56] perform pixel-wise prediction such as SCNN [26], while segmentation-based methods ignore to take the lane as a whole, resulting in insuperior performance. Anchor-based methods [7, 28, 37] regress accurate lanes by refining predefined anchors. Different from segmentation-based and anchor-based methods, parameter-based methods [19, 29] consider lane as a polynomial function and perform lane detection by regressing the parameters of the polynomial function. Since anchor-based methods are more robust and accurate than the other two methods, we implement O2SFormer based on the anchor-based method.

2.2 Label assignment in DETR

DETR [8] performs one-to-one label assignment to achieve end-to-end object detection. Recent works [9, 12, 55] have shown that one-to-one label assignment produces low training efficiency because of sparse supervision and label semantic conflicts. Group DETR [9] introduces additional queries to increase supervision. H-DETR [12] is similar to Group DETR, except that the additional queries are assigned labels by one-to-many assignment. However, introducing additional queries brings out extra computational burden during training. O2SFormer employs one-to-many assignment in the first $N-1$ decoder layers to increase supervision without introducing extra queries. DDQ [55] filters out anchors with similar label semantic as fully positive anchors by a simple class-agnostic NMS. Unlike DDQ, O2SFormer assigns layer-wise soft labels to positive lane anchors with similar label semantic as fully positive lane anchors.

3 Method

The structure of O2SFormer is shown in Fig. 2. Sec 3.1 introduces the representation of lane anchors. Sec 3.2 details the Dynamic anchor-based positional query. Sec 3.3 describes the One-to-several label assignment and layer-wise soft label.

3.1 Representation of lane anchors

Lanes have obvious shape and position priors, thus predefining lane anchors on the input image can help the model better locate the lanes. Following [37], we employ equally-spaced 2D points as the representation for lane anchors and all lane anchors are learnable. Specifically, lane anchors can be represented as a sequence of 2D points, i.e., $Anchor = \{(x_1, y_1), \dots, (x_z, y_z)\}$. The y-coordinate is uniformly sampled along the vertical edge of the image, i.e., $y_i = \frac{H}{z-1} * i$. Where z is the number of sampling points and H denotes height of the image. The x-coordinates are one-to-one corresponding to the y-coordinates. In this paper, we regress the accurate lanes by refining lane anchors. The outputs of the network consist of four components: (1) the length of the lane anchors. (2) the start point of the lane anchors and the angle between x-axis of the lane anchors (denoted as x, y and θ). (3) probabilities of background and foreground. (4) The z offsets, i.e., the horizontal distance between z sampling points and its ground truth. We first predict the background and foreground probabilities for lane anchors. Then, we obtain the start point, length and angle for foreground lane anchors. Finally, we refine foreground lane anchors by regressing z offsets.

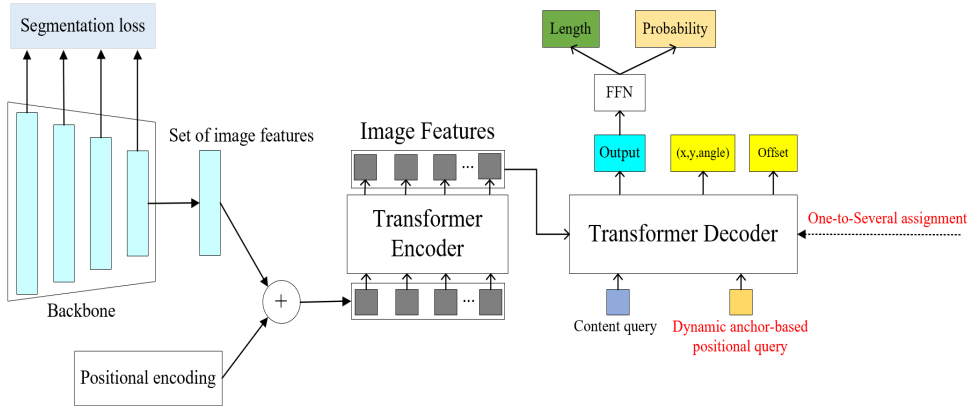


Figure 2: Pipeline of O2SFormer. O2SFormer adopts a convolutional neural network as the backbone to learn the 2D feature representation of the input image. We flatten the 2D feature representation and add positional encoding. Then, the features are fed into the Transformer Encoder. The Transformer Decoder takes the dynamic anchor-based positional query, content query and image features as inputs. We pass output embedding of the Transformer decoder to a feed forward network(FFN) that predicts background and foreground probabilities and the length of lane anchors. One-to-Several assignment is used to assign labels for lane anchors in each decoder layer.

3.2 Dynamic anchor-based positional Query

Conditional DETR [23] points that object query in DETR can be divided into content query and positional query. Content query is responsible for learning the content information of the image and positional query is used to learn location information. Conditional DETR shows that the positional query only provides the general attention map without giving explicit positional prior information, which makes network require more training epochs to learn how to locate objects. Compared with object detection, lanes have stronger positional prior. General attention makes network more difficult to learn the feature of lanes.

As illustrated in Fig. 3, dynamic anchor-based positional query aims to explore clear positional prior information. Since the length of the lane is not the main determinants of positional information, we consider the start point, angle and offset as the positional prior information of the lane. Specifically, we use $A_k = (x_k, y_k, \theta_k)$ to represent the start point coordinate and angle of the k-th lane anchor. $offset_k$ indicates z offsets of the k-th lane anchor. Dynamic anchor-based positional query is denoted as $P_k \in R^D$ and D is dimension.

In order to reduce the computational burden in the subsequent spatial positional encoding, we map $offset_k$ to a float through a multilayer perceptron (MLP). The mapped float is named with Lane Offset Embedding($LOE_k \in R$). We concatenate the LOE_k with A_k to obtain the k-th lane anchor(denoted as M_k).

$$M_k = Cat(A_k, LOE_k) \quad (1)$$

Where cat is concatenate operation. P_k can be generated by

$$P_k = MLP(PE(M_k)) \quad (2)$$

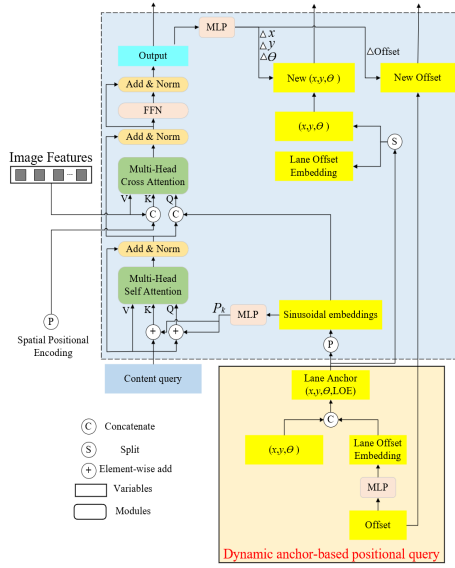


Figure 3: Structure of Decoder Layer. Q, K and V represent Query, Key and Value.

PE represents spatial positional encoding to generate sinusoidal embeddings from M_k . As M_k is a quaternion, PE is overloaded here:

$$PE(M_k) = PE(x_k, y_k, \theta_k, LOE_k) = Cat(PE(x_k), PE(y_k), PE(\theta_k), PE(LOE_k)) \quad (3)$$

In spatial positional encoding, we map a float to a vector with $D/2$ dimensions as: $R \rightarrow R^{D/2}$. MLP maps the vector generated by PE into D dimensions. All MLP modules in the decoder layer are composed of a linear layer and ReLU activation.

In multi-head self-attention, the content query (denoted as C_k) of the keys, queries, and values are the same. Queries and keys include extra position items.

$$Key_k = C_k + P_k, \quad Query_k = C_k + P_k, \quad Value_k = C_k \quad (4)$$

For multi-head cross-attention, we concatenate the content and position information as queries and keys. We use F to represent image features.

$$Query_k = Cat(C_k, PE(M_k)), \quad Key = Cat(F, PE(F)), \quad Value = F \quad (5)$$

Dynamic update of lane anchor. Since the initial lane anchors are not accurate enough, we update lane anchors layer-by-layer. In particular, as shown in Fig. 3, we use an extra MLP module to predict $(\Delta x, \Delta y, \Delta \theta, \Delta offset)$ from the output of the decoder layer. Then we split M_k to get the A_k . The new A_k and $offset_k$ are obtained as following:

$$A_k^{new} = A_k + (\Delta x, \Delta y, \Delta \theta) \quad (6)$$

$$offset_k^{new} = offset_k + \Delta offset \quad (7)$$

3.3 One-to-Several label assignment

DETR employs one-to-one assignment to achieve end-to-end detection. In one-to-one assignment, a ground truth is assigned only one positive lane anchor, while many lane anchors

with similar label semantic as positive lane anchor are assigned as negative lane anchors, resulting in label semantic conflicts. Although one-to-many assignment can effectively solve label semantic conflicts, one-to-many assignment is unable to keep end-to-end detection. Hence, we propose the One-to-Several (O2S) label assignment to alleviate label semantic conflicts while keeping end-to-end detection.

As shown in Fig. 1, we apply one-to-many assignment in the first $N-1$ decoder layers and use one-to-one assignment in the last decoder layer. Existing methods [24, 54] assign labels separately for each decoder layer, leading to inconsistent label assignment across different decoder layers. On the contrary, O2S assignment utilizes the output of the last decoder layer to assign labels for all decoder layers. Specifically, we first perform Optimal Transport Assignment(OTA) [7] on the output of the last decoder layer to get the positive lane anchors for one-to-many assignment. OTA dynamically assigns t ($t \geq 2$) positive lane anchors for each label according to the Line-IOU(LIOU) [57] between the predictions and the ground truths. Then, we perform Hungarian matching [9] on t positive lane anchors to obtain the positive lane anchor for one-to-one assignment. We define the positive lane anchor used for one-to-one assignment as the fully positive lane anchor.

Layer-wise soft label. Although the first $N-1$ decoder layers employ one-to-many assignment to address label semantic conflicts, such manner makes one-to-one assignment difficult to optimize. To elegantly combine the advantages of one-to-one and one-to-many assignment, we propose the layer-wise soft label. As illustrated in Fig. 1, we decrease the positive weights of positive lane anchors used for one-to-many assignment layer-by-layer, except the fully positive lane anchor. For the shallow layers of decoder, we assign soft label with high positive weights to positive lane anchors to enhance the ability of feature representation. In the deep layers of decoder, we assign soft label with low positive weights to positive lane anchors to make the decoder focus on one-to-one assignment. For the r -th ($1 \leq r \leq N-1$) decoder layer, the soft label of the j -th positive lane anchor is

$$d_j^r = \begin{cases} 1, & \text{if fully positive lane anchor} \\ \frac{N-r}{N-1} \times W_j, & \text{otherwise} \end{cases} \quad (8)$$

$$W_j = \frac{pred_j^r}{\max(pred_i^r)}, i \in S \quad (9)$$

Where $pred_j^r$ represents the predicted classification score of positive lane anchor j in the r -th decoder layer. We use a feed forward network to obtain $pred_j^r$ from output of the r -th decoder layer. S represents the collection of positive lane anchors for one-to-many assignment. O2SFormer filters low quality predictions by setting predicted classification score threshold, which causes that predictions with high LIOU and low predicted classification score are filtered and predictions with low LIOU and high predicted classification score are retained. Hence, we use LIOU to weight the soft label following [53]. The classification loss is formulated as

$$Loss_{cls}^r = \sum_{j \in S} FL(pred_j^r, d_j^r \times LIOU_j^r) + \sum_{j \in B} FL(pred_j^r, 0) \quad (10)$$

$$Loss_{cls} = \sum_{r=1}^{N-1} Loss_{cls}^r + FL(pred_{fully}^N, LIOU_{fully}^N) + \sum_{j \neq fully} FL(pred_j^N, 0) \quad (11)$$

Where FL is Focal loss [18]. $LIOU_j^r$ denote the LIOU of positive lane anchor j in the r -th decoder layer. $pred_{fully}^N$ and $LIOU_{fully}^N$ are predicted classification score and LIOU of fully positive lane anchor in the last decoder layer. B is the set of negative lane anchors. Regression loss of O2SFormer is

$$Loss_{reg}^r = \sum_{j \in B} \{ \lambda_{iou} \times L_{iou}(b_j^r, b_{gt}) + \lambda_{l1} \times [L_{l1}((x_j^r, y_j^r), (x_{gt}, y_{gt})) + L_{l1}(\theta_j^r, \theta_{gt}) + L_{l1}(l_j^r, l_{gt})] \} \quad (12)$$

$$Loss_{reg} = \sum_{r=1}^N Loss_{reg}^r \quad (13)$$

b_j^r , (x_j^r, y_j^r) , θ_j^r and l_j^r are predicted location of z sampling points, start point coordinate, angle and length of positive lane anchor j in the r -th decoder layer. b_{gt} , (x_{gt}, y_{gt}) , θ_{gt} and l_{gt} denote the ground truth of b_j^r , (x_j^r, y_j^r) , θ_j^r and l_j^r respectively. L_{iou} is Line-IOU loss [67] and L_{l1} is smooth-l1 loss [8]. λ_{iou} and λ_{l1} are the weight of L_{iou} and L_{l1} . Besides, we adopt segmentation loss as an auxiliary loss following [67]. The total loss of O2SFormer is

$$Loss = \lambda_{cls} \times Loss_{cls} + Loss_{reg} + \lambda_{seg} \times Loss_{seg} \quad (14)$$

Where λ_{cls} and λ_{seg} are the weight of classification loss and segmentation loss respectively. We take the Cross entropy loss as the segmentation loss.

4 Experiment

4.1 Experimental Setting

Dataset. We evaluate O2SFormer on the CULane dataset [76]. CULane is a widely used large-scale dataset for lane detection. It contains a lot of challenging scenarios such as crowded roads. The CULane dataset consists of 88.9K images for training, 9.7K images in the validation set, and 34.7K images for the test. Image size is 1640×590.

Evaluatoin Metrics. We adopt the F1 score to measure the performance on CULane: $F1 = \frac{2 \times Precision \times Recall}{Precision + Recall}$, where $Precision = \frac{TP}{TP + FP}$ and $Recall = \frac{TP}{TP + FN}$. FP , TP and FN are false positives, true positives and false negatives respectively.

4.2 Implementation Details

We adopt ResNet [10] pretrained on ImageNet [6] as the backbone. All images are resized to 320×800. For data augmentation, we use random horizontal flips and random affine transforms(translation, rotation and scaling). We utilize AdamW [20] optimizer with learning rate of 2.5e-4. Cosine decay strategy is applied to update learning rate. We train 20 epochs on CULane. All experiments are conducted on 2 GPUs. O2SFormer is implemented based on MMDetection [9]. We set the number of sampling points z to 72 and the number of lane anchors to 192. λ_{cls} , λ_{iou} , λ_{l1} and λ_{seg} are set to 2, 2, 0.3 and 1 respectively. The initial value of z offsets are set to 0. We initialize the position of lane anchors following [67]. All feed forward networks in O2SFormer consist of three MLP modules.

4.3 Comparison with Existing methods

Main results. The performance of O2SFormer on CULane testing set is shown in Table 1. O2SFormer achieves the best results among Transformer-based detectors. For example, O2SFormer(ResNet18) outperforms the Laneformer(ResNet18) in total F1 score(76.07% vs 71.71%). With ResNet18, O2SFormer surpasses LSTR by a great margin (76.07% vs 64.00%). Compared with CNN-based detectors, O2SFormer with ResNet50 is superior to LaneATT with a large ResNet122 backbone in terms of F1 score and MACs(77.83% vs 77.02%, 27.51G vs 86.5G). Moreover, O2SFormer achieves the better performance in hard scenarios like Dazzle and Night. Visual results can be found in the supplementary materials.

Analysis on convergence speed. We show the comparison of convergence speed between O2SFormer and DETR in Fig. 4. Fig. 4 shows that O2SFormer converges 12.5× faster than DETR.

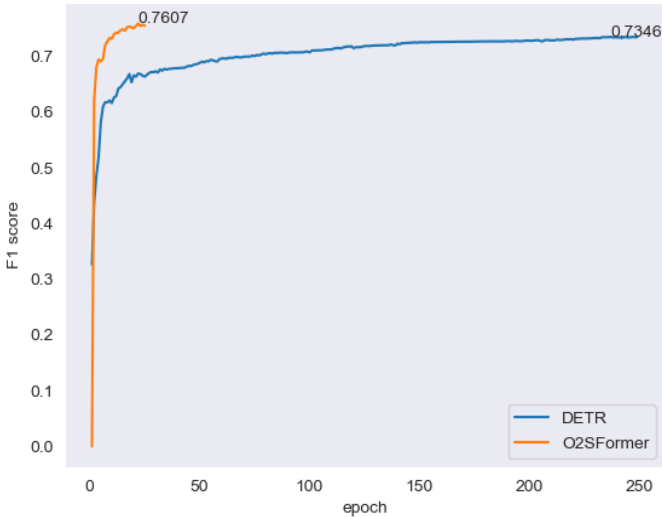


Figure 4: Convergence curves for O2SFormer and DETR. Two models are trained with ResNet18. O2SFormer converges much faster than DETR.

Table 1: Comparison of F1 score and MACs(multiply-accumulate operations) on CULane testing set. * represents O2SFormer with hybrid-encoder used in RT-DETR [22]. We report false positives for “Cross” category.

Methods	Normal	Crowded	Dazzle	Shadow	No line	Arrow	Curve	Night	Cross	Total	MACs(G)
LSTR(ResNet18) [15]	-	-	-	-	-	-	-	-	-	64.00	-
SCNN(ResNet50) [24]	90.60	69.70	58.50	66.90	43.40	84.10	64.40	66.10	1900	71.60	-
UFLD(ResNet34) [25]	90.70	70.20	59.50	69.30	44.40	85.70	69.50	66.70	2037	72.30	-
PINet(Hourglass) [16]	90.30	72.30	66.30	68.40	49.80	83.70	65.20	67.70	1427	74.40	-
CurveLane-L [26]	90.70	72.30	67.70	70.10	49.40	85.80	68.40	68.90	1746	74.08	86.5
LaneATT(ResNet122) [27]	91.74	76.16	69.47	76.31	50.46	86.29	64.05	70.81	1264	77.02	70.5
Laneformer(ResNet18) [8]	88.60	69.02	64.07	65.02	45.00	81.55	60.46	64.76	25	71.71	13.8
Laneformer(ResNet50) [8]	91.77	75.74	70.17	75.75	48.73	87.65	66.33	71.04	19	77.06	26.2
O2SFormer(ResNet18)	91.89	73.86	70.40	74.84	49.83	86.08	68.68	70.74	2361	76.07	15.21
O2SFormer(ResNet34)	92.50	75.25	70.93	77.72	50.97	87.63	68.10	72.88	2749	77.03	25.05
O2SFormer(ResNet50)	93.09	76.57	72.25	76.56	52.80	89.50	69.60	73.85	3118	77.83	27.51
O2SFormer(ResNet50)*	93.89	82.03	80.29	83.89	71.46	92.11	76.21	80.48	3208	78.00	43.11

4.4 Ablation study

In this section, we ablate the key components in O2SFormer. If not specific, we adopt O2SFormer with ResNet18 for all ablation experiments and results are shown in Table 2. More ablation studies can be found in supplementary materials.

Table 2: Ablation study results of key components of O2SFormer on CULane. FPS is test on a single 2080Ti GPU with TensorRT.

Methods	Epoch	F1(%)	Precision(%)	Recall(%)	FPS	Params(M)
DETR	250	73.46	79.26	61.79	89	30.9
+Dynamic anchor-based positional query	50	74.09	81.11	62.28	84	31.1
+One-to-Several label assignment	20	75.20	82.88	65.39	84	31.1
+Layer-wise soft label	20	76.07	83.92	65.94	84	31.1

Effectiveness of Dynamic anchor-based positional query. As we can see in Table 2, directly applying DETR in lane detection only obtains 73.46% F1 score. The add of Dynamic

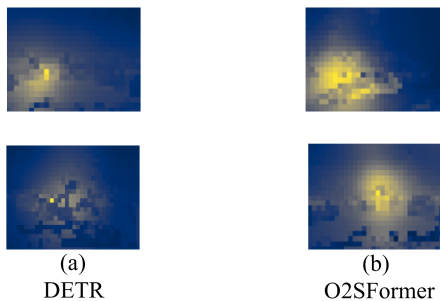


Figure 5: We visual the positional attention maps of positional queries for DETR and O2SFormer with similar query position. Following [20], we perform dot product between positional embeddings from a feature map and a positional query to calculate the attention map.

anchor-based positional query improves the F1 score from 73.46% to 74.09%. The precision and recall are increased by 1.85%(81.11% vs 79.26%) and 0.49%(62.28% vs 61.79%). We also visual few positional attention maps of positional queries in Fig. 5. Compared with positional attention map of DETR, the positional attention map of O2SFormer has a more clear focus area. Above results demonstrate that Dynamic anchor-based positional query can effectively improve the model performance.

Effectiveness of One-to-several label assignment. One-to-one label assignment in DETR results in label semantic conflicts while one-to-many label assignment needs NMS to remove duplicate predictions. We propose one-to-several assignment to combine the advantages of both label assignments. As shown in Table 2, equipped with one-to-several assignment, F1 score gains 1.11%(75.20% vs 74.09%) improvements and recall is increased by 3.11%(65.39% vs 62.28%). It should be noted that one-to-several label assignment spends fewer training epochs achieving better performance.

Effectiveness of layer-wise soft label. We futher explore the impact of layer-wise soft label. Layer-wise soft label delivers a 0.87% F1 score improvements(76.07% vs 75.20%) and increases the precision by 1.04%(83.92% vs 82.88%). Since layer-wise soft label is used in training, it has no influence on FPS and parameters.

5 Conclusion

In this paper, we present the One-to-Several Transformer(O2SFormer) to achieve end-to-end lane detection. Through one-to-several label assignment, we enable the detectors to address label semantic conflicts and keep end-to-end detection at the same time. We assign layer-wise soft label to positive lane anchors to achieve the balance between one-to-one and one-to-many assignment. To explore explicit positional prior information, we propose the dynamic anchor-based positional query by encoding lane anchors as positional queries. Experimental results show that O2SFormer significantly speeds up the convergence of DETR and surpasses Transformer-based and CNN-based detectors on the CULane dataset. In the future, we will focus on applying one-to-several label assignment to CNN-based detectors.

References

- [1] Amol Borkar, Monson Hayes, and Mark T Smith. A novel lane detection system with efficient ground truth generation. *IEEE Transactions on Intelligent Transportation Systems*, 13(1):365–374, 2011.
- [2] Nicolas Carion, Francisco Massa, Gabriel Synnaeve, Nicolas Usunier, Alexander Kirillov, and Sergey Zagoruyko. End-to-end object detection with transformers. In *Computer Vision—ECCV 2020: 16th European Conference, Glasgow, UK, August 23–28, 2020, Proceedings, Part I 16*, pages 213–229. Springer, 2020.
- [3] Kai Chen, Jiaqi Wang, Jiangmiao Pang, Yuhang Cao, Yu Xiong, Xiaoxiao Li, Shuyang Sun, Wansen Feng, Ziwei Liu, Jiarui Xu, Zheng Zhang, Dazhi Cheng, Chenchen Zhu, Tianheng Cheng, Qijie Zhao, Buyu Li, Xin Lu, Rui Zhu, Yue Wu, Jifeng Dai, Jingdong Wang, Jianping Shi, Wanli Ouyang, Chen Change Loy, and Dahua Lin. MMDetection: Open mmlab detection toolbox and benchmark. *arXiv preprint arXiv:1906.07155*, 2019.
- [4] Qiang Chen, Xiaokang Chen, Gang Zeng, and Jingdong Wang. Group detr: Fast training convergence with decoupled one-to-many label assignment. *arXiv preprint arXiv:2207.13085*, 2022.
- [5] Zhenpeng Chen, Qianfei Liu, and Chenfan Lian. Pointlanenet: Efficient end-to-end cnns for accurate real-time lane detection. In *2019 IEEE intelligent vehicles symposium (IV)*, pages 2563–2568. IEEE, 2019.
- [6] Jia Deng, Wei Dong, Richard Socher, Li-Jia Li, Kai Li, and Li Fei-Fei. Imagenet: A large-scale hierarchical image database. In *2009 IEEE conference on computer vision and pattern recognition*, pages 248–255. Ieee, 2009.
- [7] Zheng Ge, Songtao Liu, Zeming Li, Osamu Yoshie, and Jian Sun. Ota: Optimal transport assignment for object detection. In *Proceedings of the IEEE/CVF Conference on Computer Vision and Pattern Recognition*, pages 303–312, 2021.
- [8] Ross Girshick. Fast r-cnn. In *Proceedings of the IEEE international conference on computer vision*, pages 1440–1448, 2015.
- [9] Jianhua Han, Xiajun Deng, Xinyue Cai, Zhen Yang, Hang Xu, Chunjing Xu, and Xiaodan Liang. Laneformer: Object-aware row-column transformers for lane detection. In *Proceedings of the AAAI Conference on Artificial Intelligence*, volume 36, pages 799–807, 2022.
- [10] Kaiming He, Xiangyu Zhang, Shaoqing Ren, and Jian Sun. Deep residual learning for image recognition. In *Proceedings of the IEEE conference on computer vision and pattern recognition*, pages 770–778, 2016.
- [11] Yuenan Hou, Zheng Ma, Chunxiao Liu, and Chen Change Loy. Learning lightweight lane detection cnns by self attention distillation. In *Proceedings of the IEEE/CVF international conference on computer vision*, pages 1013–1021, 2019.
- [12] Ding Jia, Yuhui Yuan, Haodi He, Xiaopei Wu, Haojun Yu, Weihong Lin, Lei Sun, Chao Zhang, and Han Hu. Detsr with hybrid matching. *arXiv preprint arXiv:2207.13080*, 2022.

- [13] Heechul Jung, Junggon Min, and Junmo Kim. An efficient lane detection algorithm for lane departure detection. In *2013 IEEE Intelligent vehicles symposium (IV)*, pages 976–981. IEEE, 2013.
- [14] Kang Kim and Hee Seok Lee. Probabilistic anchor assignment with iou prediction for object detection. In *Computer Vision—ECCV 2020: 16th European Conference, Glasgow, UK, August 23–28, 2020, Proceedings, Part XXV 16*, pages 355–371. Springer, 2020.
- [15] Yeongmin Ko, Younkwan Lee, Shoaib Azam, Farzeen Munir, Moongu Jeon, and Witold Pedrycz. Key points estimation and point instance segmentation approach for lane detection. *IEEE Transactions on Intelligent Transportation Systems*, 23(7):8949–8958, 2021.
- [16] Minhyeok Lee, Junhyeop Lee, Dogyoon Lee, Woojin Kim, Sangwon Hwang, and Sangyoun Lee. Robust lane detection via expanded self attention. In *Proceedings of the IEEE/CVF winter conference on applications of computer vision*, pages 533–542, 2022.
- [17] Xiang Li, Jun Li, Xiaolin Hu, and Jian Yang. Line-cnn: End-to-end traffic line detection with line proposal unit. *IEEE Transactions on Intelligent Transportation Systems*, 21(1):248–258, 2019.
- [18] Tsung-Yi Lin, Priya Goyal, Ross Girshick, Kaiming He, and Piotr Dollár. Focal loss for dense object detection. In *Proceedings of the IEEE international conference on computer vision*, pages 2980–2988, 2017.
- [19] Ruijin Liu, Zejian Yuan, Tie Liu, and Zhiliang Xiong. End-to-end lane shape prediction with transformers. In *Proceedings of the IEEE/CVF winter conference on applications of computer vision*, pages 3694–3702, 2021.
- [20] Shilong Liu, Feng Li, Hao Zhang, Xiao Yang, Xianbiao Qi, Hang Su, Jun Zhu, and Lei Zhang. Dab-detr: Dynamic anchor boxes are better queries for detr. *arXiv preprint arXiv:2201.12329*, 2022.
- [21] Ilya Loshchilov and Frank Hutter. Decoupled weight decay regularization. *arXiv preprint arXiv:1711.05101*, 2017.
- [22] Wenyu Lv, Shangliang Xu, Yian Zhao, Guanzhong Wang, Jinman Wei, Cheng Cui, Yuning Du, Qingqing Dang, and Yi Liu. Detsr beat yolos on real-time object detection. *arXiv preprint arXiv:2304.08069*, 2023.
- [23] Depu Meng, Xiaokang Chen, Zejia Fan, Gang Zeng, Houqiang Li, Yuhui Yuan, Lei Sun, and Jingdong Wang. Conditional detr for fast training convergence. In *Proceedings of the IEEE/CVF International Conference on Computer Vision*, pages 3651–3660, 2021.
- [24] Sandipann P Narote, Pradnya N Bhujbal, Abhilasha S Narote, and Dhiraj M Dhane. A review of recent advances in lane detection and departure warning system. *Pattern Recognition*, 73:216–234, 2018.

- [25] Jianwei Niu, Jie Lu, Mingliang Xu, Pei Lv, and Xiaoke Zhao. Robust lane detection using two-stage feature extraction with curve fitting. *Pattern Recognition*, 59:225–233, 2016.
- [26] Xingang Pan, Jianping Shi, Ping Luo, Xiaogang Wang, and Xiaoou Tang. Spatial as deep: Spatial cnn for traffic scene understanding. In *Proceedings of the AAAI Conference on Artificial Intelligence*, volume 32, 2018.
- [27] Zequn Qin, Huanyu Wang, and Xi Li. Ultra fast structure-aware deep lane detection. In *Computer Vision—ECCV 2020: 16th European Conference, Glasgow, UK, August 23–28, 2020, Proceedings, Part XXIV 16*, pages 276–291. Springer, 2020.
- [28] Lucas Tabelini, Rodrigo Berriel, Thiago M Paixao, Claudine Badue, Alberto F De Souza, and Thiago Oliveira-Santos. Keep your eyes on the lane: Real-time attention-guided lane detection. In *Proceedings of the IEEE/CVF conference on computer vision and pattern recognition*, pages 294–302, 2021.
- [29] Lucas Tabelini, Rodrigo Berriel, Thiago M Paixao, Claudine Badue, Alberto F De Souza, and Thiago Oliveira-Santos. Polylanenet: Lane estimation via deep polynomial regression. In *2020 25th International Conference on Pattern Recognition (ICPR)*, pages 6150–6156. IEEE, 2021.
- [30] Yue Wang, Dinggang Shen, and Eam Khwang Teoh. Lane detection using spline model. *Pattern Recognition Letters*, 21(8):677–689, 2000.
- [31] Hang Xu, Shaoju Wang, Xinyue Cai, Wei Zhang, Xiaodan Liang, and Zhenguo Li. Curvelane-nas: Unifying lane-sensitive architecture search and adaptive point blending. In *Computer Vision—ECCV 2020: 16th European Conference, Glasgow, UK, August 23–28, 2020, Proceedings, Part XV 16*, pages 689–704. Springer, 2020.
- [32] Jiaying Yang, Lihe Zhang, and Huchuan Lu. Lane detection with versatile atrousformer and local semantic guidance. *Pattern Recognition*, 133:109053, 2023.
- [33] Haoyang Zhang, Ying Wang, Feras Dayoub, and Niko Sunderhauf. Varifocalnet: An iou-aware dense object detector. In *Proceedings of the IEEE/CVF Conference on Computer Vision and Pattern Recognition*, pages 8514–8523, 2021.
- [34] Shifeng Zhang, Cheng Chi, Yongqiang Yao, Zhen Lei, and Stan Z Li. Bridging the gap between anchor-based and anchor-free detection via adaptive training sample selection. In *Proceedings of the IEEE/CVF conference on computer vision and pattern recognition*, pages 9759–9768, 2020.
- [35] Shilong Zhang, Jiaqi Wang, Jiangmiao Pang, Chengqi Lyu, Wenwei Zhang, Ping Luo, Kai Chen, et al. Dense distinct query for end-to-end object detection. *arXiv preprint arXiv:2303.12776*, 2023.
- [36] Tu Zheng, Hao Fang, Yi Zhang, Wenjian Tang, Zheng Yang, Haifeng Liu, and Deng Cai. Resa: Recurrent feature-shift aggregator for lane detection. In *Proceedings of the AAAI Conference on Artificial Intelligence*, volume 35, pages 3547–3554, 2021.
- [37] Tu Zheng, Yifei Huang, Yang Liu, Wenjian Tang, Zheng Yang, Deng Cai, and Xiaofei He. Clrnet: Cross layer refinement network for lane detection. In *Proceedings of the IEEE/CVF conference on computer vision and pattern recognition*, pages 898–907, 2022.

Appendix

In this appendix, we provide more training details(Appendix A), ablation studies(Appendix B) and visualization results(Appendix C) on CULane dataset.

A More training details

Following [37], the cost of OTA includes classification cost C_{cls} and similarity cost C_{sim} . The total cost is defined as:

$$Cost = w_{sim} \times C_{sim} + w_{cls} \times C_{cls} \quad (15)$$

$$C_{sim} = (C_{dis} \times C_{xy} \times C_{theta})^2 \quad (16)$$

Here we take the focal cost [18] between predictions and labels as C_{cls} . C_{sim} contains three components, C_{dis} denotes the average distance between valid sampling points and ground truth, C_{xy} means the distance of the start point between predictions and ground truth, C_{theta} means the difference of the angle between predictions and ground truth. We normalize the C_{theta} to $[0,1]$. w_{cls} And w_{sim} are the weight of classification cost and similarity cost. We set w_{sim} and w_{cls} to 3 and 1 respectively. Besides, we set the number of decoder layer N to 6.

B More ablation studies

In this section, we provide more ablation study results to confirm the effectiveness of O2SFormer. If not specific, we still adopt the ResNet18 as the backbone.

Table 3: Results of number of lane anchors.

Number of lane anchors	F1(%)	MACs(G)
4	68.25	11.92
16	71.48	12.13
64	73.69	12.97
192	76.07	15.21
256	76.10	16.34
512	76.28	20.82

Number of lane anchors. We ablate the number of lane anchors and results are shown in Table 3. Since there are at most 4 lanes in a image, we increase the number of lane anchors from 4 to 512. We can obviously observe that as the number of lane anchors increases, F1 score improves significantly. When number of lane anchors is 256 or 512, MACs is increased from 15.21G to 16.34G or 20.82G, whereas F1 score improves slightly. Hence, we set the number of lane anchors to 192.

Table 4: Performances of different one-to-many label assignments.

Method	F1(%)	Precision(%)	Recall(%)
ATSS [34]	74.21	81.59	64.77
PAA [14]	75.19	82.76	65.98
OTA [10]	76.07	83.92	65.94

Performances of different one-to-many label assignments. Table 4 compares different one-to-many label assignments. We can see that OTA achieves better performance than the

other two label assignments in terms of F1 score and Precision. Therefore, we adopt the OTA as the one-to-many label assignment in O2SFormer.

C Visualization results on CULane

In Fig.6, we visualize the detection results of O2SFormer on CULane. O2SFormer can effectively detect lanes under various scenarios.

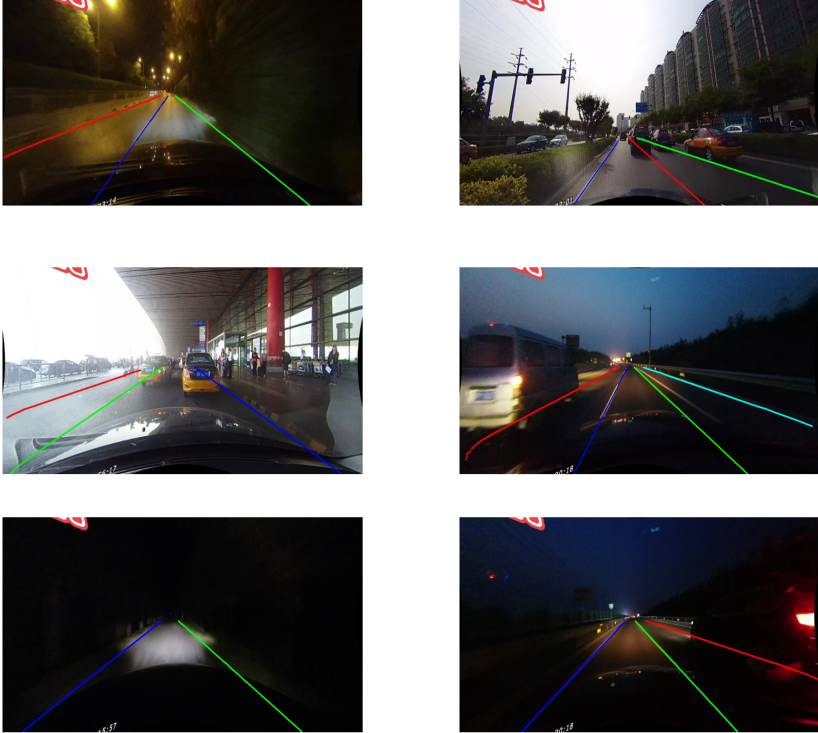


Figure 6: Viusalization results on CULane.